

## Abstract and Introduction

In future, GNSS data streams with high data rates up to 1 Hz or even more will be used in many GNSS RTK applications or high precision geophysical applications. In these analyses it is generally assumed that the original GNSS observations are stochastically uncorrelated and that they can be modelled adequately by diagonal co-variance matrices. This may be valid for observations that are typically sampled every 30 sec or more. However, in high rate applications these assumptions of the stochastic model of GNSS observations should be revised.

A prominent source for physical correlations of GNSS phase observations are refractivity fluctuations within the troposphere. Depending on the prevailing atmospheric and turbulent conditions, the wind direction and wind speed as well as the changing satellite-receiver geometry different correlation patterns occur. In the following, the impact of different atmospheric parameters on correlations lengths is shown both theoretically and based on real GNSS data.

## Temporal stochastic behaviour of tropospheric delays

Atmospheric turbulence is characterised as a non-stationary stochastic process. An appropriate tool to assess the temporal behaviour of a non-stationary process  $X$  is the temporal structure function (Wheelon 2001):

$$D_X(\tau) = \langle [X(t+\tau) - X(t)]^2 \rangle \quad (1)$$

with  $\langle \rangle$  denoting an ensemble average and  $\tau$  indicating the time lag between two values of  $X$ .

An explicit expression for the temporal structure function of phase measurements  $\varphi$  (and tropospheric delays  $T$ ) is provided by (Wheelon 2001) as follows (for parameter descriptions see Tab. 1):

$$D_\varphi(\tau) = D_T(\tau) = 1.564 R k^2 C_n^2 \kappa_0^{-5/3} \times \left( 1 - 0.995 (\kappa_0 v \tau)^{5/6} K_{5/6}(\kappa_0 v \tau) \right) \quad (2)$$

Figure 1 shows the explicit temporal structure function, Eq. 2, for various typical turbulence parameter sets evaluated for a fixed geometry with an elevation of  $13.5^\circ$ .

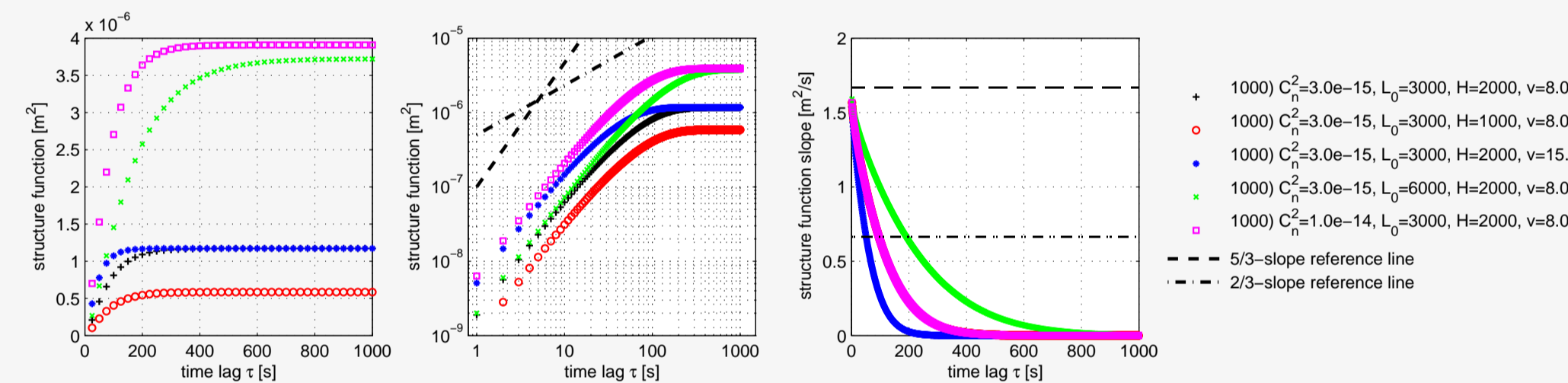


Figure 1: Explicit temporal structure functions of slant tropospheric delays for typical atmospheric turbulence

Logarithmic plots of explicit temporal structure functions show an approximate 5/3 power-law behaviour for the first  $\approx 80$  s. Depending on the specified turbulence parameters (especially the outer scale length  $L_0$ ) a continuous decrease of the exponent can be seen. At a maximum of approximately 600 s the exponent reaches zero (for these examples), i.e., the measurements can be considered as uncorrelated.

Variable:	Description:	Variable:	Description:
$C_n^2$	Structure constant of refractivity	$v_0$	Wind velocity
$\kappa_0 = 2\pi/L_0$	Turbulence wavenumber to corresponding outer scale length $L_0$	$d$	Separation distance between actual integration points
$k = 2\pi/\lambda$	Electromagnetic wavenumber	$H$	Height of wet troposphere
$\alpha_v$	Wind direction (azimuth)	$\varepsilon_A^i$	Elevation of satellite $i$ at station $A$
$\epsilon_v$	Wind direction (elevation)	$T_A^i$	Slant tropospheric delay at station $A$ to satellite $i$
$K$	modified Bessel function of 2. kind	$R$	Length of propagation path

Table 1: Parameter descriptions for Eq. (2) and (3)

## Covariance expression of slant tropospheric delays

A general co-variance expression for tropospheric delays has been derived by Schön and Brunner (2008) (for parameter descriptions see Tab. 1):

$$\langle T_A^i, T_B^j \rangle = 0.31 \frac{\kappa_0^{-2/3}}{\sin \varepsilon_A^i \sin \varepsilon_B^j} C_n^2 \times \int_0^H \int_0^H (\kappa_0 d)^{1/3} K_{-1/3}(\kappa_0 d) dz_1 dz_2 \quad (3)$$

Using real or simulated observation geometries as well as adequate turbulence parameters a fully occupied variance-covariance matrix  $\Sigma_T$  of tropospheric delays can be set up to generate simulated tropospheric delay variations  $\mathbf{T}$  via an eigenvalue decomposition of  $\Sigma_T = \mathbf{GAG}^{-1}$  and  $\mathbf{T} = \mathbf{G}\sqrt{\Lambda}\mathbf{x}$  ( $\mathbf{x}$  is a vector of Gaussian random numbers with zero mean and unit variance).

## Simulated and real tropospheric delay variations

Figures 2 and 3 each show five realisations of simulated slant delays for a rising satellite and a (stationary) zenith satellite using typical turbulence parameters. Using a sampling rate of 0.1 Hz the simulation periods yield 1000 and 100 observations, respectively. For the rising satellite scenario (Fig. 2) variations in the range of  $\pm 2$  mm are observed. The temporal structure functions show an initial power-law behaviour of slightly less than 5/3 that quickly decreases. For time shifts larger than 300 s the simulated slant delays can be considered as uncorrelated.

For the zenith satellite scenario (Fig. 3) smaller variations in the range of less than  $\pm 1$  mm can be seen. The temporal structure functions show a similar behaviour with an initial power-law behaviour of almost 5/3 that quickly decreases to  $\approx 2/3$  with a (mean) correlation time of approximately 250-300 s.

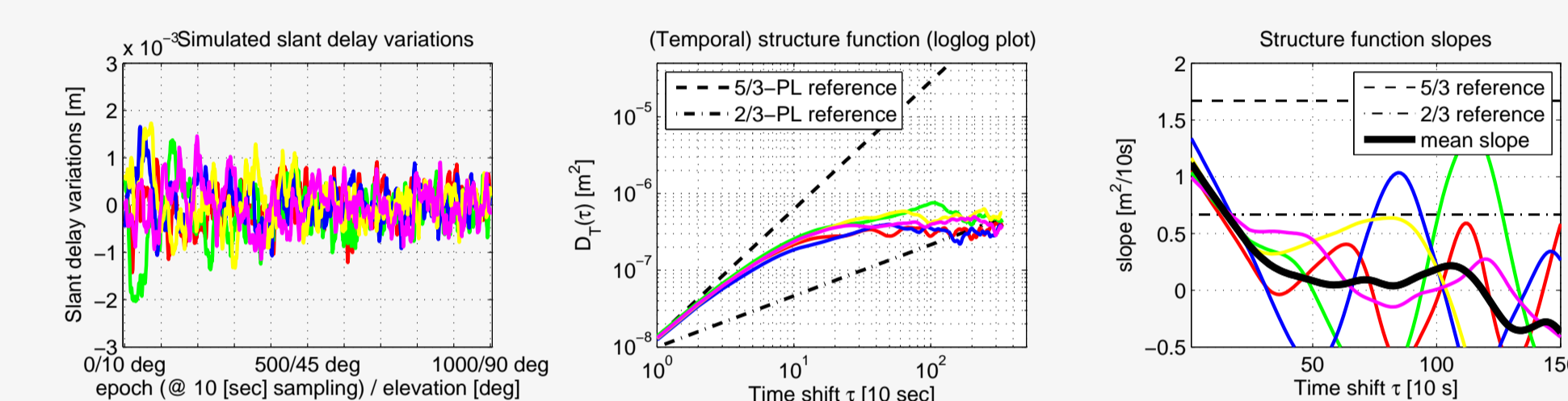


Figure 2: Simulated slant delay variations for a satellite rising from  $10^\circ$  to  $90^\circ$  using average turbulence parameters

$$(C_n^2 = 0.3 \times 10^{-14} \text{ m}^{-2/3}, L_0=3000 \text{ m}, H=2000 \text{ m}, v=8 \text{ m/s}, \alpha_v=0^\circ)$$

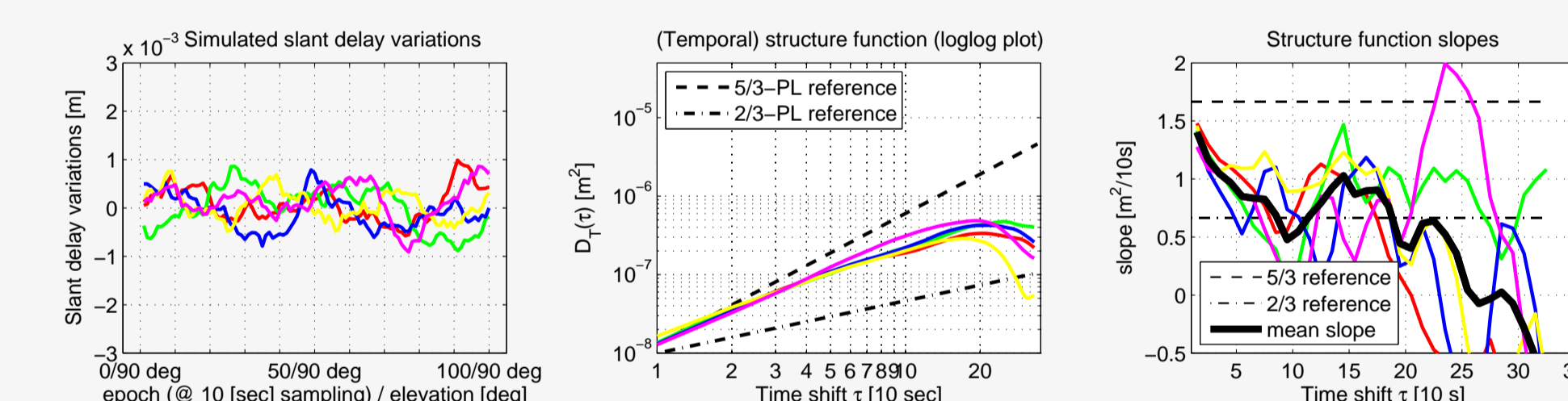


Figure 3: Simulated delay variations for a (stationary) zenith satellite using average turbulence parameters

$$(C_n^2 = 0.3 \times 10^{-14} \text{ m}^{-2/3}, L_0=3000 \text{ m}, H=2000 \text{ m}, v=8 \text{ m/s}, \alpha_v=0^\circ)$$

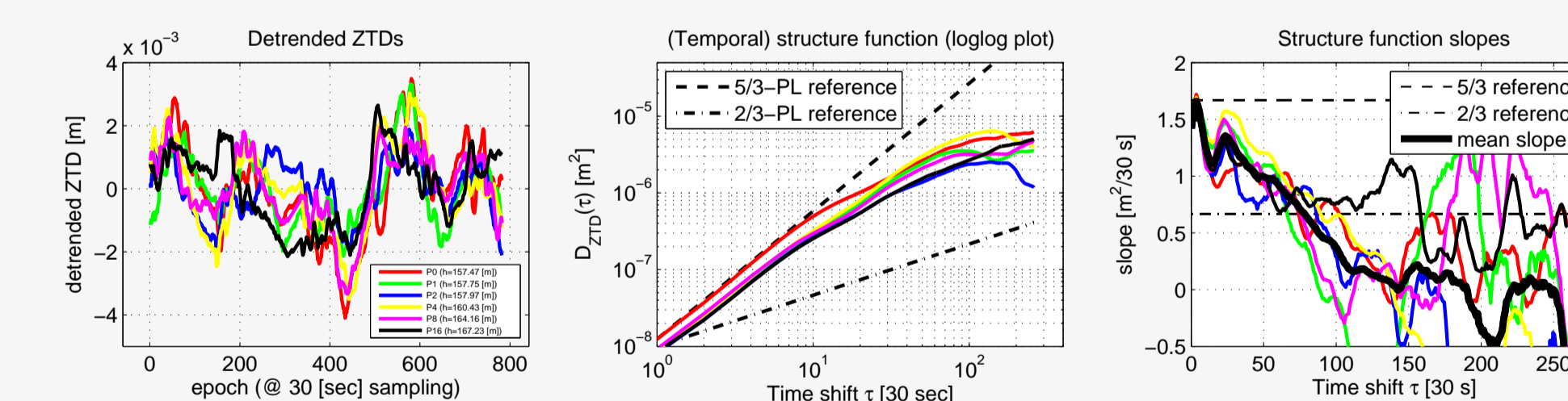


Figure 4: Real zenith delay variations for a network consisting of six GPS receivers P0-P16 located along a 16 km straight line (station names P.x indicate the distance  $x$  from the first antenna P0, local obs. time: 10:30-16:30)

Real zenith tropospheric delay variations (Fig. 4) from a PPP solution also show an initial 5/3 power-law behaviour which continuously decreases with a mean correlation time of about 3000 s. Further investigations concentrate on the analysis of these effects (e.g., caused by pressure and temperature variations).

## References & Acknowledgements

- Schön S, Brunner FK: Atmospheric turbulence theory applied to GPS carrier-phase data, J Geod 82(1): 47-57, 2008.  
 Vennebusch M, Schön S: Generation of slant tropospheric delay time series based on turbulence theory, Geodesy for Planet Earth-IAG 2009.  
 Wheelon AD: Electromagnetic scintillation-I. Geometrical optics, Cambridge University Press, Cambridge, 2001.

The authors thank the German Research Foundation (Deutsche Forschungsgemeinschaft) for its financial support (SCHO 1314/1-1).